Effects of Aged Wooden Members on Seismic Performance of Old Traditional Wooden Structures

Y. Ooka, H. Tanahashi, K. Izuno, Y. Suzuki & K. Toki
Ritsumeikan University, Japan

SUMMARY:
This paper examined the seismic performance of existing old traditional wooden structures in consideration of aging of wooden members by means of strength tests, embedment tests and nonlinear earthquake response analysis. As a result of strength tests, most of aged members have similar or larger Young's moduli and strengths compared to new ones. The embedment tests show that Elasto-plastic Pasternak Model (abbreviated to EPM) simulation is available to evaluate the embedment characteristics of aged members. The nonlinear earthquake response analysis was conducted for Kiyomizu temple model by using EPM formulation. The results showed that the response acceleration of the building increased a little by reflecting the stiffness and embedment characteristic of old zelkova. However, the safety of the building was confirmed.

Keywords: traditional wooden structure, aging, EPM formulation, nonlinear earthquake response analysis

1. INTRODUCTION

There are many old traditional wooden temples, shrines and town houses recognized as invaluable cultural heritage in Japan. As big earthquakes occur frequently in Japan, it is very important to protect the cultural heritage from earthquakes. In order to establish the seismic evaluation of such buildings, the aging effects of old wooden materials are also important. Thus, the object of this research is to evaluate the seismic performance of an existing old traditional wooden structure, Kiyomizu temple, as shown in Fig. 1.1 in consideration of aged wooden members.

(a) Main hall

(b) Stage

Figure 1.1. Kiyomizu temple (World heritage site by UNESCO)

Many kinds of wood species are used for the structural members of Japanese traditional wooden structures. Zelkova (*Keyaki*), Japanese cedar (*Sugi*: described "cedar" in this paper), Japanese cypress (*Hinoki*: described "cypress" in this paper) and Japanese red pine (*Akamatsu*: described "red pine" in this paper) are popular species. The stiffness and strength change of wood with aging depends on the species. For example, the stiffness and strength of cypress and red pine continues to increase for hundreds of years after emplacement, then, decreases gradually. But zelkova wood begins to lose stiffness and strength after emplacement [Hirashima et al., 2004a, 2004b, 2005, Kohara, 2003]. The reason of this different tendency due to wood species is that the advance balance of crystallization and chemical disintegration of cellulose which constitute a wood is different by wood species [Kohara, 2003]. However, the strength properties of old members are not clear due to lack of data so far.

First, strength and embedment tests were conducted to evaluate the strength and embedment properties of old wooden members. Second, the embedment tests were simulated based on the proposed Elasto-plastic Pasternak Model (abbreviated to EPM) [Tanahashi et al., 2011a] and assumed the restoring force characteristics of joints. Last, numerical simulation was conducted for Kiyomizu temple by means of nonlinear earthquake response analysis in consideration of the test results and the results simulated are discussed.

2. STRENGTH TESTS OF AGED MEMBERS

The compression test and bending test were conducted in order to evaluate the stiffness and strength of old members.

2.1. Test method

The compression and bending tests were conducted according to Japanese Industrial Standards [JISZ2101, 2009]. Each test specimen for the compression test was a rectangular solid with a cross section of 30mm by 30mm and a length of 60mm. On the other hand, Each test specimen for the bending test was a rectangular solid with a cross section of 20mm by 20mm and a length of 320mm (Span length: 280mm). After conducting the tests, we calculated Young's modulus (compression: $\boldsymbol{E_c}$, bending: $\boldsymbol{E_b}$) and strength (compression: $\boldsymbol{\sigma_c}$, bending: $\boldsymbol{\sigma_b}$).
The aged woods; zelkova, cedar, cypress and red pine were obtained from Japanese traditional wooden buildings. These specimens were obtained from structural members that had been in place for 90 (cedar <Ce90>, red pine <P90>), 130 (cypress <Cy130>), 155 (red pine <P155>), 167 (zelkova <Z167>), 170 (cedar <Ce170>, red pine <P170>), 189 (zelkova <Z189>, cedar <Ce189>), 220 (zelkova <Z220>), 300 (red pine <P300>), 320 (cypress <Cy320>) and 375 (zelkova <Z375>, cypress <Cy375>) years. These wood ages were measured by carbon dating. Elapsed years of structural members were holistically judged from the wood age and construction age of the buildings. The numbers of test specimens are shown in Tables 2.1 and 2.2.

Table 2.1. Numbers of test specimens (zelkova, cedar)

species	zelkova					cedar			
elasped years	0	167	189	220	375	0	90	170	189
symbol	Z0	Z1670	Z189	Z220	Z375	Ce0	Ce90	Ce170	Ce189
compression	6	4	6	12	12	36	-	9	6
bending	6	4	6	-	-	-	6	8	6

Table 2.2. Numbers of test specimens (cypress, red pine)

species	cypress				red pine				
elasped years	0	130	320	375	0	90	155	170	300
symbol	Cy0	Cy130	Cy320	Cy375	P0	P90	P155	P170	P300
compression	18	-	-	24	6	-	12	10	10
bending	6	6	6	3	6	6	15	8	7

Some specimens were not obtained from the aged wood due to their bad conditions. In Tables 2.1 and 2.2, Z0, Ce0, Cy0 and P0 means new zelkova, cedar, cypress and red pine specimens, respectively.

2.2. Results of strength test

The relation between the average test results and elapsed years are shown in Figs. 2.1, 2.2, 2.3 and 2.4. In these figures, the determination coefficient R^2 of correlation between density and each test results are added. Also, the average values of database in Handbook [Forestry and Forest Products Research Institute, 2004] are added.
Figs. 2.1, 2.2, 2.3 and 2.4 show that correlation of density and each test result is small except $\boldsymbol{E_c}$ of cypress and $\boldsymbol{\sigma_c}$ of cedar. Thus, the differences in test results among different ages might be chiefly attributable to aging phenomena. Moreover, it turned out that the change with aging of the test results in compression and bending are similar.

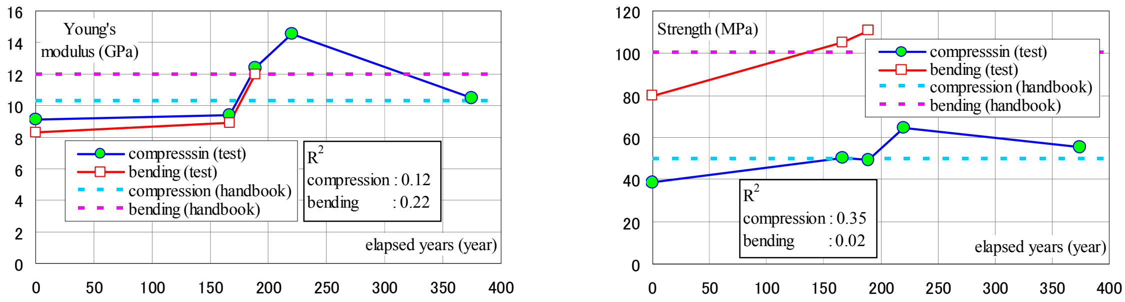

(a) Young's modulus (b) strength

Figure 2.1. Zelkova

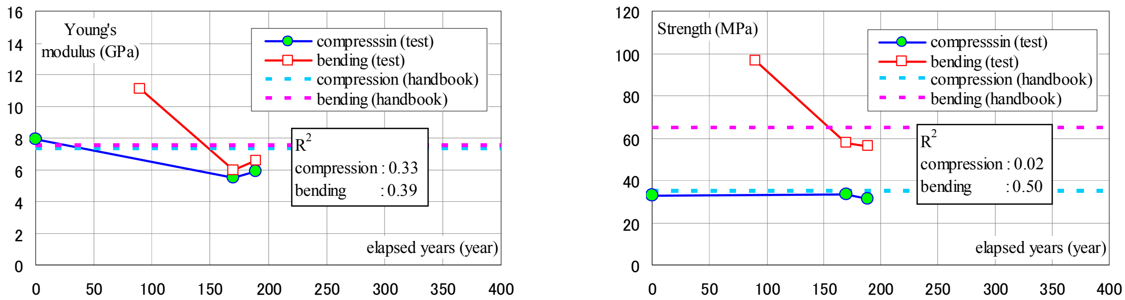

(a) Young's modulus (b) strength

Figure 2.2. Cedar

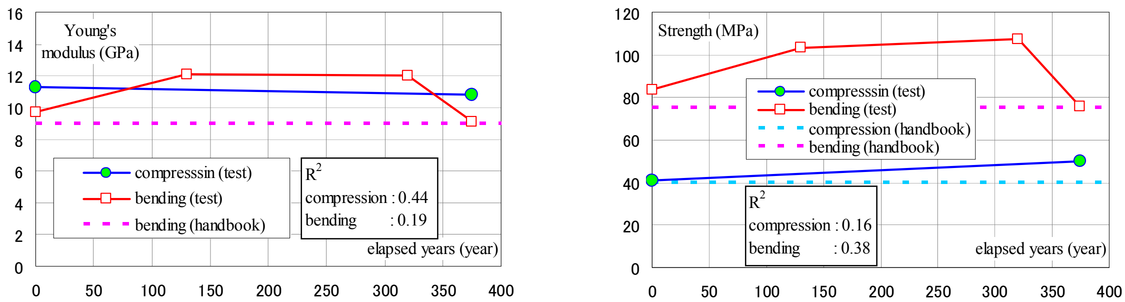

(a) Young's modulus (b) strength

Figure 2.3. Cypress

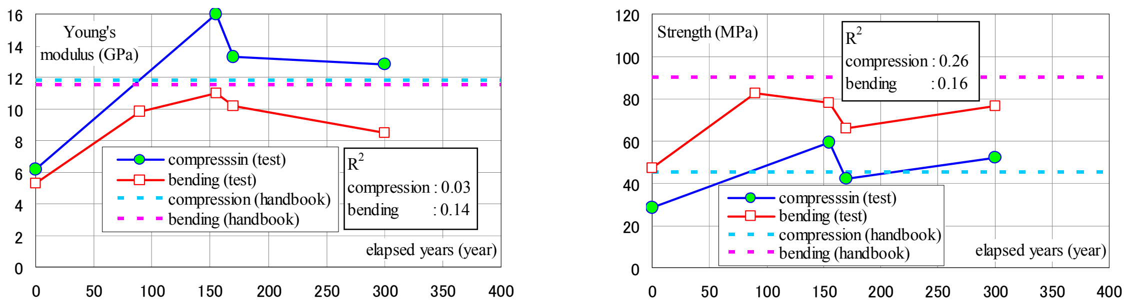

(a) Young's modulus (b) strength

Figure 2.4. Red pine

In zelkova wood, old zelkova has greater Young's modulus and strength than new woods. E_c of Z220 is larger than the other ones and E_b of Z189 is largest. The results show that Young's modulus of zelkova increase for 220 years after emplacement. This change tendency is the same also in strength. Unlike zelkova, new cedar has a higher Young's modulus and strength than old woods. However, the value of old cedar is not so low as compared with those of Handbook. Cypress and red pine have the similar tendency as zelkova. As a result, most of aged members have similar or larger Young's moduli and strengths compared to new ones. However, some of the bending specimens of old zelkova and Japanese red pine tended to show brittle failure.

3. EMBEDMENT TESTS FOR AGED MEMBERS

The embedment characteristics of existing aged wooden members are essential for accurate evaluation of seismic performance of Japanese traditional wooden structures. It is because the rotational resistance of traditional wooden joints plays the most important role among the seismic elements of traditional wooden structures. In order to evaluate them accurately, the embedment tests was conducted for the same wood species of strength tests.

3.1. Test method

We used the same embedment test method as referred literature [Tanahashi et al., 2011a], which is shown in Fig. 3.1. The embedment test specimen consists of one partial compression specimen (P) and two full compression specimens (S) cut from both sides of the partial one in the longitudinal direction to reduce the variations among these specimens. And all specimens were compressed with rigid steel plates. The size of partial compression specimen was 2L=30mm, 2H=30mm and ΔL=30mm. In this test, test specimens were classified according to the three directions of annual rings as shown in Fig. 3.2, since embedment characteristics change greatly with the loading direction. The legend of LR means the radial loading direction, LT; tangential, and LTR; annual ring angle α =45° between LR and LT of cross section respectively. The numbers of test specimens are shown in Tables 3.1 and 3.2.

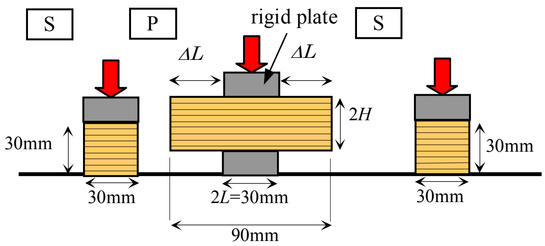

Figure 3.1. Embedment test method

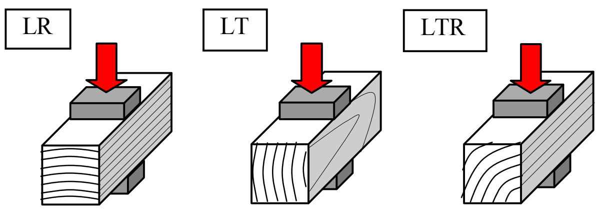

Figure 3.2. Direction of annual ring

Table 3.1. Numbers of test specimens (zelkova, cedar)

species	zelkova				cedar		
elapsed years	0	167	189	375	0	170	189
symbol	Z0	Z1670	Z189	Z375	Ce0	Ce170	Ce189
embedment (LR.LT.LTR)	6.6.6	3.3.4	6.6.6	0.0.8	12.12.12	6.6.6	6.6.6

Table 3.2. Numbers of test specimens (cypress, red pine)

species	cypress		red pine			
elapsed years	0	375	0	155	170	300
symbol	Cy0	Cy375	P0	P155	P170	P300
embedment (LR.LT.LTR)	18.18.18	3.3.6	6.6.6	4.4.4	6.6.6	3.2.2

3.2. Test results

Fig. 3.3 shows stress-strain relations of P155-LTR (P1, S1 and S2). Fig. 3.3 shows that the stiffness of partial compression specimen is greater than that of full compression specimen. This phenomenon is important feature of wood embedding perpendicular to the grain. Therefore, the embedment properties of old members were evaluated by using the "Elasto-plastic Pasternak Model" (abbreviated to EPM) simulation [Tanahashi et al., 2011a]. We can simulate the elasto-plastic restoring force characteristics of partial compression simply using the stiffness function which considers the strain softening/hardening behavior of lateral compression and the EPM parameters $\boldsymbol{E}$, $\boldsymbol{\varepsilon_y}$ ($\boldsymbol{\sigma_y}$), $\boldsymbol{\gamma H}$, $\boldsymbol{\eta}$, $\boldsymbol{C}$. $\boldsymbol{E}$

and ε_y were the averages of Young's moduli and yield strains in lateral compression obtained by using the inter-crosshead strains of two full compression test specimens on both sides of the partial test specimen. The other parameters were determined as follows. The non-dimensional characteristic value γH was calculated by the ratio of stiffness in the results of the full and partial compression tests. As for γH, the smaller this value is, the greater the increasing ratio of stiffness is. The yield strain ratio η and constant C were also determined in order to agree with the post-yield stiffness. Fig. 3.4 shows the EPM simulation results for P155-LTR (P1, S1 and S2).

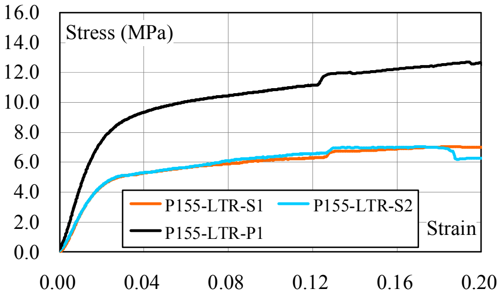

Figure 3.3. Stress-strain relation (P155-LTR)

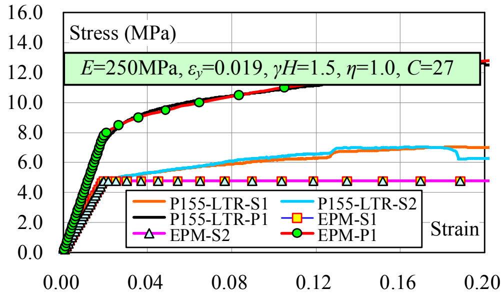

Figure 3.4. EPM simulation (P155-LTR)

The average values of the EPM parameters are shown in Tables 3.3 and 3.4. Young's modulus $\boldsymbol{E}$ and yield stress $\boldsymbol{\sigma_y}$ of aged zelkova are small compared with new ones. The characteristic values $\boldsymbol{\gamma H}$ of Z167 is rather smaller than those of Z0 and Z189 in all directions of annual ring angles. The parameters $\boldsymbol{\eta}$ are similar for new and aged wood. In cedar, $\boldsymbol{E}$ and $\boldsymbol{\sigma_y}$ of Ce170 is larger than those of Ce0 and Ce189. For cypress, most of aged wood have similar or larger $\boldsymbol{E}$ and $\boldsymbol{\sigma_y}$ compared with new ones. There are little differences in other parameters of new and aged wood. The change of $\boldsymbol{E}$ and $\boldsymbol{\sigma_y}$ of red pine due to aging are similar to those of Japanese cypress. However, it is difficult to evaluate the difference in new and aged wood since the variations of parameter $\boldsymbol{\gamma H}$ and $\boldsymbol{C}$ are high.

Table 3.3. EPM parameters (zelkova, cedar)

spesimen	annual ring direction	E (MPa)	ε_y	γH	η	C	σ_y (MPa)
Z0	LR	1508	0.010	5.2	1.2	22	14.78
	LT	983	0.013	3.7	1.1	23	12.54
	LTR	942	0.011	4.2	1.1	23	10.53
Z167	LR	995	0.013	3.5	1.1	21	12.66
	LT	888	0.014	2.4	1.2	29	12.18
	LTR	900	0.014	4.1	1.1	23	12.10
Z189	LR	1179	0.012	5.9	1.2	42	14.29
	LT	885	0.015	5.8	1.2	41	13.22
	LTR	831	0.015	4.8	1.2	40	12.31
Z375	LR	-	-	-	-	-	-
	LT	-	-	-	-	-	-
	LTR	674	0.011	3.0	1.1	50	7.66
Ce0	LR	325	0.006	2.9	1.2	24	1.98
	LT	347	0.012	2.5	1.2	53	4.18
	LTR	88	0.022	1.1	1.4	19	1.73
Ce170	LR	511	0.009	2.8	1.2	43	4.67
	LT	295	0.018	2.4	1.2	42	5.21
	LTR	288	0.018	2.0	1.2	25	4.15
Ce189	LR	358	0.007	2.7	1.2	17	2.63
	LT	259	0.015	1.7	1.2	70	3.98
	LTR	67	0.020	1.0	1.1	5	1.33

Table 3.4. EPM parameters (cypress, red pine)

spesimen	annual ring direction	E (MPa)	ε_y	γH	η	C	σ_y (MPa)
Cy0	LR	638	0.009	2.9	1.2	36	5.70
	LT	350	0.017	2.2	1.3	49	5.76
	LTR	197	0.021	1.5	1.3	36	3.76
Cy375	LR	383	0.016	2.9	1.1	27	6.10
	LT	420	0.020	2.5	1.2	82	8.51
	LTR	260	0.019	2.2	1.1	25	4.78
P0	LR	904	0.006	4.5	1.3	37	5.57
	LT	500	0.014	4.0	1.3	29	7.08
	LTR	226	0.014	2.2	1.2	23	3.11
P155	LR	821	0.007	5.1	1.0	36	5.37
	LT	528	0.016	2.5	1.3	42	8.02
	LTR	415	0.014	2.1	1.0	36	5.13
P170	LR	732	0.008	4.2	1.1	87	5.81
	LT	457	0.015	3.8	1.4	41	6.95
	LTR	436	0.014	3.0	1.0	52	4.98
P300	LR	900	0.009	5.9	1.0	60	7.73
	LT	523	0.016	1.7	1.2	65	8.36
	LTR	395	0.015	5.5	1.1	29	5.69

In all test results, Tables 3.3 and 3.4 show that the parameter $\boldsymbol{\eta}$ are constant about 1.0 to 1.4, and the parameters $\boldsymbol{C}$ highly vary between 5 and 87, whose characteristics should be researched in further studies. However, the tendency is found that parameters $\boldsymbol{C}$ are large in the brittle specimens because of small plastic stiffness. Furthermore, the tendency is found that the characteristics values $\boldsymbol{\gamma H}$ and yield stress $\boldsymbol{\sigma_y}$ depend on Young's modulus $\boldsymbol{E}$. The determination coefficient R^2 of $\boldsymbol{E}$ and $\boldsymbol{\gamma H}$ is 0.50, and the value of $\boldsymbol{E}$ and $\boldsymbol{\sigma_y}$ is 0.76.

4. NUMERICAL SIMULATIONS

The numerical analysis was conducted to figure out the effect of aging on the earthquake response of the heritage structure. In this chapter, the aging effect of the Young's modulus and embedment characteristics on the earthquake response was evaluated using EPM formulation.

4.1. Objective Structure

Kiyomizu temple in Kyoto was chosen as an objective structure of this simulation. This temple was first built in 805, and was reconstructed in 1633 following a fire in 1629. As it is located on a steep hillside, a large open-air stage is attached to the main hall. The dimension of the building is 40m by 36m wide and 18m high, and the stage columns are 13m high at the maximum. A main structural member of Kiyomizu temple is zelkova. Figs. 4.1 and 4.2 show cross-sectional and plan view of the building. Japanese wooden temples of this type are constructed without using nails or other metal devices at joints.

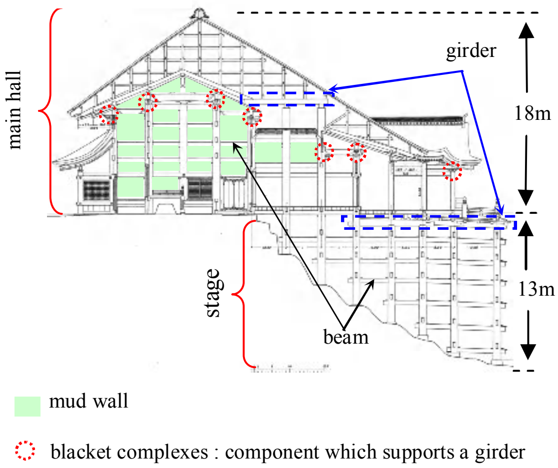

Figure 4.1. Cross-sectional view

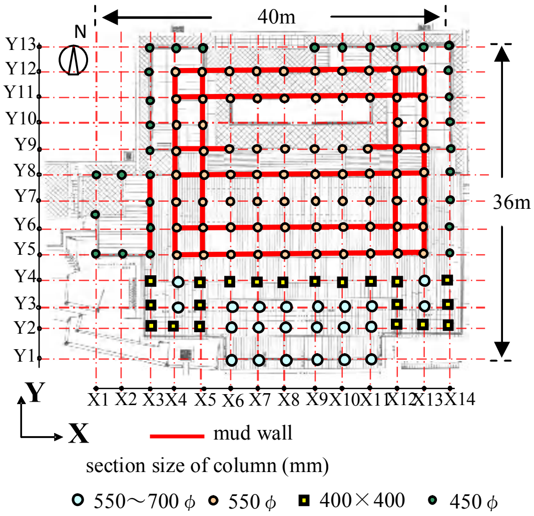

Figure 4.2. Plan view

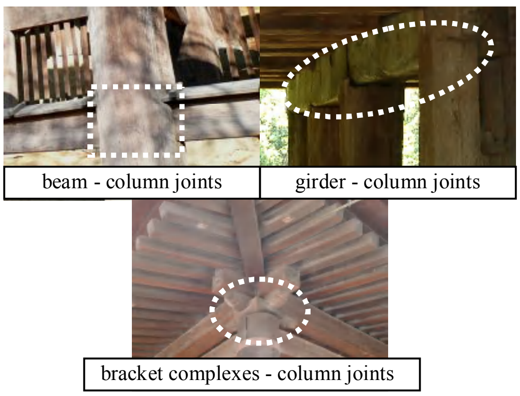

Figure 4.3. Wooden joints

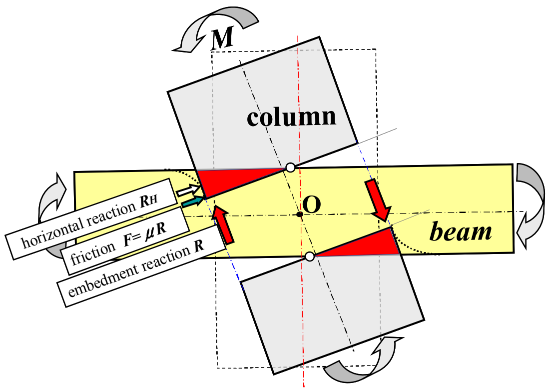

Figure 4.4. Rotational embedment of beam-column joint

4.2. Numerical model

A previously developed numerical analysis model for Kiyomizu temple [Suzuki et al., 2007] was used to verify the seismic performance of the building based on the results of strength and embedment tests of old zelkova. In the numerical model, joints and mud walls were modeled as nonlinear springs, while columns, beams, and girders as elastic members. This temple has many traditional wooden joints;

beam-column joints, girder-column joints and bracket complexes-column joints. These joints are shown in Fig. 4.3. Important structural wood mechanisms in traditional structures are the restoring force of the rotational resistances of semi-rigid joints due to embedding at contact interfaces within wooden joints as shown in Fig. 4.4.

4.3. Mecahnical properties of aged zelkova joints

The changed parts in the present numerical model by considering aged zelkova woods were Young's modulus and the hysteretic model of wooden joints. Young's modulus was assumed by the results of strength test. And we calculated the hysteretic model of wooden joints by using EPM formulation for cross type beam-column joints [Tanahashi et al., 2011b]. The EPM formulation can calculate a hysteretic model of beam column joints including post-yield stiffness by using parameters (***E***, $\boldsymbol{\varepsilon_y}$ ($\boldsymbol{\sigma_y}$), $\boldsymbol{\gamma H}$, $\boldsymbol{\eta}$, ***C***) and $\boldsymbol{\mu}$ (coefficient of friction between wood). In this model, ***E*** and $\boldsymbol{\varepsilon_y}$ were reflected by the results of embedment tests of old zelkova and the other parameters were referred to Tanahashi et al., [2011b]. Since there are no data of ***E*** of LR and LT directions, the value of LTR direction of Z0, Z167, Z189 and Z375 were used. For a half of girder-column joints and bracket complexes-column joints, the yield moment and rotational stiffness also were assumed to be the half of beam-column joints. Table 4.1 shows parameters of the simulation of each old zelkova and Fig. 4.5 shows a hysteretic model of beam-column joints in consideration of aging.

Table 4.1. Parameters of simulation

spesimen	E_c (GPa)	EPM parameters					
		E (MPa)	ε_y	γH	η	C	μ
Z0	9.1	942	0.011	5.23	2.43	15.5	0.50
Z167	9.4	900	0.014	5.10			
Z189	12.4	831	0.015	4.89			
Z376	10.5	674	0.011	4.42			

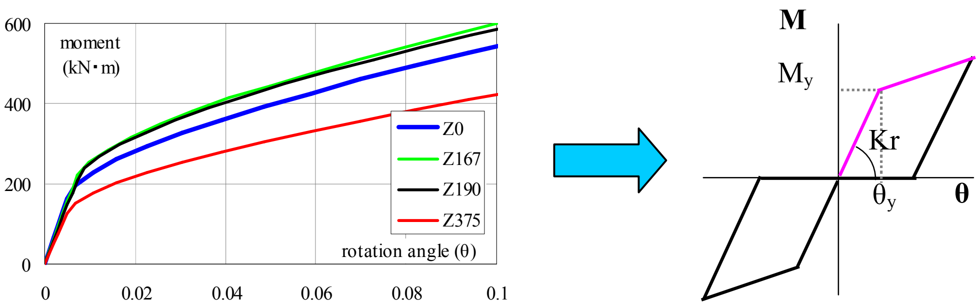

(a) Aging change of spring property (b) Hysteretic model

Figure 4.5. Assumed hysteretic model of beam-column joints

4.4. Natural Periods

The calculated natural periods are shown in Table 4.2. The natural periods of Z167 and Z375 are found to be similar to the value of Z0. Since Young's modulus of Z189 is largest, the natural periods of Z189 became shorter in 90% of another.

Table 4.2. Natural Periods (s)

case	Z0	Z167	Z189	Z375
First mode (N-S)	0.52	0.51	0.47	0.50
Second mode (E-W)	0.44	0.44	0.41	0.44
Third mode (rotation)	0.24	0.24	0.22	0.23

4.5. Input Earthquake Motion and Analysis

The input earthquake waves used for nonlinear earthquake response analysis were the Hanaore wave (maximum acceleration: EW-1033cm/s^2, NS-929cm/s^2) and JMA Kobe wave with the maximum velocity of 50kine (maximum acceleration: EW-521cm/s^2, NS-469cm/s^2). Hanaore wave is an assumed earthquake wave at Hanaore fault in Kyoto, which is supposed to cause the worst influence on Kiyomizu temple [Toki et al., 2007]. JMA kobe 50kine wave is a normalized wave of 1995 Kobe earthquake which is used as very rare and strong earthquake. Nonlinear earthquake response analysis was conducted using Newmark's β method (β=1/4). The integration time increment was 0.002 seconds and the damping factor was set to 5% as stiffness proportional damping based on the fundamental vibration mode.

4.6. Analysis Results

The maximum angle responses of the columns at the building center for Hanaore wave are shown in Fig. 4.6, while Fig. 4.7 shows those for JMA Kobe wave. Since a limit state of Japanese traditional wooden structures is not prescribed, the serviceability limit state set to 1/120 rad and the ultimate limit state set to 1/30 rad, which is the same as common wooden residence [The building standard law, 2007].
Fig. 4.6 shows that there is no big change in consideration of stiffness and embedment spring change due to ages in both directions. There are no frames which exceed 1/30. In JMA Kobe wave, the maximum angle of Z189 is larger than the other ones (110% of Z0, Z167 and Z375). However, a big change of the angle is not found in JMA Kobe wave. For the reason that aged wood has small influence for the angle, it is thought many mud walls are arranged with sufficient balance in this building.

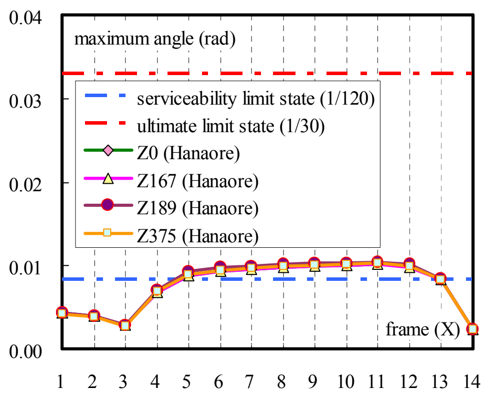

(a) N-S direction

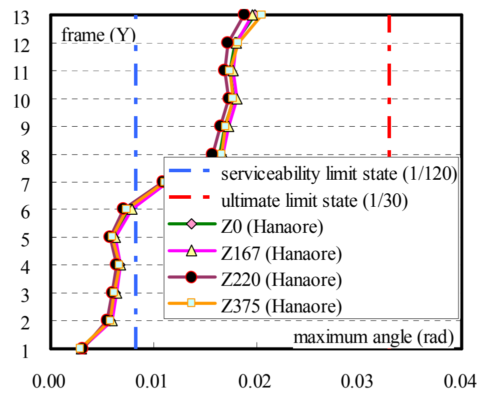

(b) E-W direction

Figure 4.6. Maximum angle of columns at individual frames (Hanaore)

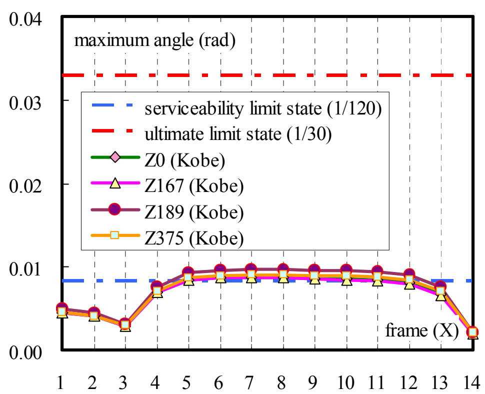

(a) N-S direction

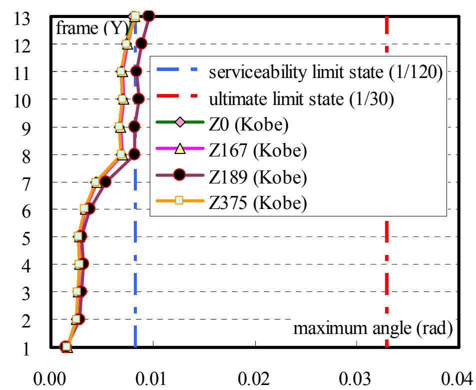

(b) E-W direction

Figure 4.7. Maximum angle of columns at individual frames (JMA Kobe 50kine)

Fig. 4.8 shows the acceleration-time histories for Hanaore wave, while Fig. 4.9 shows those for JMA Kobe wave. The response acceleration was plotted for X7 frame and Y9 frame near the building center. X7 frame shows the response in the N-S direction, and Y9 frame shows that in the E-W direction. Fig. 4.8 shows that the maximum response of Z189 is larger than another one in both directions (about 116% of Z0). In JMA Kobe wave, the maximum response is not change by aging in N-S direction, while the maximum response of Z189 is the largest in E-W direction. Fig. 4.10 shows the acceleration-time histories at edge of the stage. In Hanaore wave, the maximum response of Z189 is larger than another one (about 115% of Z0). Since numerous visitors often present on the stage, stiffness and embedding property change will have an effect on visitors.

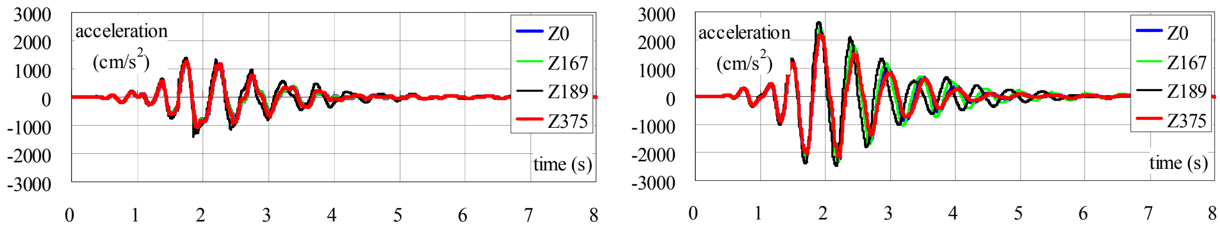

(a) N-S direction (b) E-W direction

Figure 4.8. Acceleration-time histories (Hanaore wave)

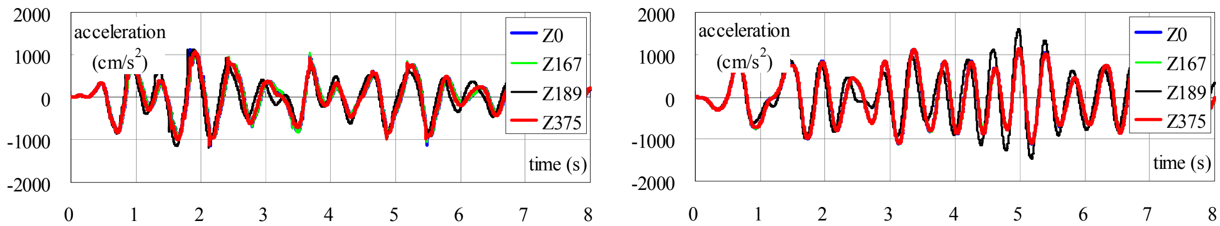

(a) N-S direction (b) E-W direction

Figure 4.9. Acceleration-time histories (JMA Kobe wave)

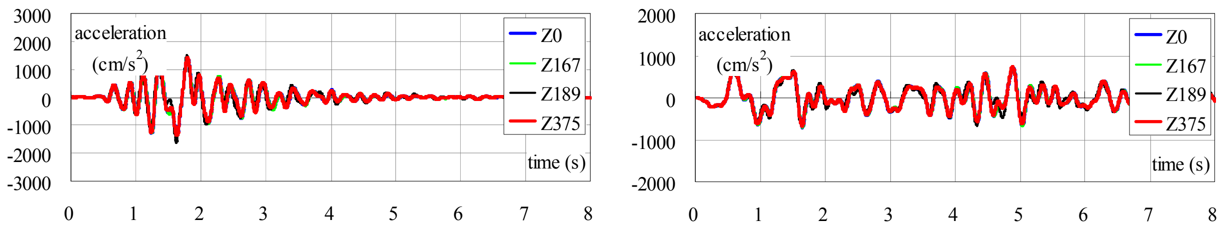

(a) Hanaore wave (b) JMA Kobe wave

Figure 4.10. Acceleration-time histories (Edge of the stage)

5. CONCLUSION

This paper studied the effect of strength and embedment property change by ages of structural members on the earthquake response of a Japanese traditional wooden temple in Kyoto. The major results obtained in this study are as follows.

1. Most of old woods have large or similar Young's moduli and strengths comparing to new ones. Moreover, it turned out that aging change of compression and bending are similar.
2. As for the EPM simulation results, the EPM parameter $\boldsymbol{\eta}$ are constant about 1.0 to 1.4, and the parameters $\boldsymbol{C}$ highly vary between 5 and 87. The tendency is found that the characteristics values $\boldsymbol{\gamma H}$ and yield stress $\boldsymbol{\sigma_y}$ depend on Young's modulus $\boldsymbol{E}$. The determination coefficient R^2 of $\boldsymbol{E}$ and

γH is 0.50, and the value of $\boldsymbol{E}$ and $\boldsymbol{\sigma_y}$ is 0.76.

3. Nonlinear earthquake response analysis by using EPM formulation shows that the change with aging of Young's modulus and embedment property of zelkova affected little on the maximum response angle of columns of Kiyomizu temple. On the other hand, these aged change had influence on response acceleration of the building. There were no frames which exceed 1/30 and the building was confirmed to be safe again.

ACKNOWLEDGEMENTS

We thank the Kiyomizu staff for providing the old wood specimens. This study was supported in part by Global COE Program, "Ritsumeikan University Global COE for Education, Research and Development of Strategy on Disaster Mitigation of Cultural Heritage and Historic Cities", MEXT, Japan and by the Grant-in-Aid for Scientific Research (S) from Japan Society for the Promotion of Science [No.19106010].

REFERENCES

Forestry and Forest Products Research Institute. (2004). *Handbook for Japanese industrial wood*. (in Japanese).

Hirashima, Y., Sugihara, M., Sasaki, Y., Ando, Y. and Yamasaki, M. (2004a). Strength properties of aged wood. Tensile strength properties of aged Keyaki and Akamatsu woods. *Journal of Wood Science* **50:5**, 301-309. (in Japanese).

Hirashima, Y., Sugihara, M., Sasaki, Y., Ando, Y. and Yamasaki, M. (2004b). Strength properties of aged wood. Compressive strength properties, shearing strength and hardness of aged Keyaki and Akamatsu woods. *Journal of Wood Science* **50:6**, 368-375. (in Japanese).

Hirashima, Y., Sugihara, M., Sasaki, Y., Ando, Y. and Yamasaki, M. (2005). Strength properties of aged wood. Static and impact bending strength prperties of aged Keyaki and Akamatsu woods. *Journal of Wood Science* **51:3**, 146-152. (in Japanese).

Japanese Standards Association. (2009). Methods of test for woods. JISZ2101. (in Japanese).

Kohara, J. (2003). Study on Wooden Culture. *NHK books*. (in Japanese).

Suzuki, T., Kurakata, M., Izuno, K. and Toki, K. (2007). Effect of stage on earthquake response of a Japansese tradtional wooden structure. *Journal of Japan Association for earthquake Engineering* **7:5**, 15-30. (in Japanese).

Tanahashi, H., Ooka, Y., Izuno, K. and Suzuki, Y. (2011a). Yielding mechanism of embedment of wood and formulation of elasto-plastic embedded displacements. *J. Struct. Constr.Eng.*, AIJ, **76:662**, 811-819. (in Japanese).

Tanahashi, H. and Suzuki, Y. (2011b). Characteristics of elasto-plastic rotational embedment of traditional wooden joints and formulation of crosspiece joints. *J. Struct. Constr.Eng.*, AIJ, **76:667**, 1675-1684. (in Japanese).

Toki, K., Kishimoto, H., Fukukawa, H. and Sakai, H. (2007). Strong ground motion prediction based on 3-dimensional non-elastic FEM in Kyoto basin area from a scenario earthquake of the Hanaore fault. *Journal of Japan Association for earthquake Engineering* **7:5**, 45-59. (in Japanese).

The building standards law. (2007). *Information Center for building Administration*. (in Japanese).